Magnetic Interactions between Rare-Earth Ions in Insulators. I. Accurate Electron-Paramagnetic-Resonance Determination of Gd^{3+} Pair-Interaction Constants in $LaCl_3$†

M. T. HUTCHINGS,* R. J. BIRGENEAU,* AND W. P. WOLF
Hammond Laboratory, Yale University, New Haven, Connecticut
(Received 10 October 1967)

A series of experiments is described which illustrate an accurate method of measuring both isotropic and anisotropic interactions between pairs of similar magnetic ions. The method is applicable whenever there are sufficient admixtures of the pair states by anisotropic interactions or crystal-field terms and the effective spin of each ion is greater than $\frac{1}{2}$. These conditions are well illustrated by Gd^{3+} neighbors in $LaCl_3$. Paramagnetic-resonance measurements at 25 and 9 GHz have been made on crystals of $LaCl_3$ containing about 1% Gd^{3+} at temperatures between 1.6 and 360°K, and a large number of weak lines have been identified as due to transitions in isolated nearest-neighbor and next-nearest-neighbor pairs. Detailed analyses of both spectra show that the interactions for both types of pairs are well represented by isotropic (Heisenberg) terms $J\mathbf{S}_1\cdot\mathbf{S}_2$, plus magnetic-dipole coupling appropriate to the separation between the neighbors. For the nearest neighbors we find $J_{nn}=0.01330$ cm^{-1} (antiferromagnetic) at 20°K, decreasing to 0.01254 cm^{-1} at 360°K; while for the next-nearest neighbors $J_{nnn}=-0.0602$ cm^{-1} (ferromagnetic) at 20°K increasing to -0.0532 cm^{-1} at 360°K. (Below 20°K somewhat increased linewidths precluded accurate measurements, but the parameters appeared to remain virtually unchanged.) Neither the magnitudes nor the signs of these values can be explained by present superexchange theories, but they are in generally good agreement with values deduced from the bulk properties of concentrated $GdCl_3$, and they resolve an ambiguity in the earlier analyses. The observed magnetic-dipole interaction parameters are also found to vary somewhat with temperature, and this may be used to estimate changes in the mean separation between neighbors due to thermal expansion. These estimates may then be combined with the observed temperature variations of the J's to deduce approximate separation dependences for J_{nn} and J_{nnn}. Both are found to be very marked ($\sim r^{13}$ and r^{22}, respectively) and appreciably more rapid than the recently proposed tenth-power law for superexchange.

1. INTRODUCTION

IN this paper, and in two subsequent papers referred to as II and III, we report the experimental investigation of magnetic and electrostatic interactions between two types of rare-earth ions in the hexagonal trichloride lattice. These experiments use the technique of electron-spin resonance from coupled pairs of ions in a diamagnetic host. This work has been carried out simultaneously with measurements on the bulk magnetic properties of the rare-earth chlorides, and the results of both types of experiment will be related. Preliminary accounts of different parts of this work have been reported previously.[1–5]

The hexagonal trichlorides were chosen as a suitable system for these investigations because of their simple structure, small cation spacing (~4.5 Å), and the availability of good single crystals of both concentrated and dilute samples. The simplicity of structure has also led to an increasing amount of theoretical interest in these compounds,[6] and there is now considerable evidence that rare-earth ions may be coupled with each other by a number of different mechanisms arising from the large unquenched orbital moments.

In addition to the usual isotropic superexchange and magnetic-dipole interactions one may generally expect to find appreciable contributions from anisotropic exchange,[7] electric quadrupole,[8] and higher multipole interactions,[9] coupling via virtual phonon exchange,[10] and cross terms involving several of these. In most cases these interactions will be much weaker than those in the more extensively investigated 3*d* and 5*d* transition metal compounds, partly because of shielding effects and partly because of larger ionic separations, but paradoxically this makes the interactions more readily measurable, as we shall see. There are two principal reasons for this: firstly, the splittings produced by weak interactions tend to be comparable with readily obtainable microwave frequencies, and standard electron-paramagnetic-resonance (EPR) techniques can thus be used to study the transitions. Secondly, the presence of several competing interactions relaxes selection rules, which in simpler

† Work supported in part by the U. S. Atomic Energy Commission.

* Present address: Clarendon Laboratory, Oxford, England.

[1] M. T. Hutchings and W. P. Wolf, in *Proceedings of the International Conference on Magnetism, Nottingham, 1964* (Institute of Physics and The Physical Society, London, 1964), p. 342.

[2] R. J. Birgeneau, M. T. Hutchings, and R. N. Rogers, Phys. Rev. Letters **16**, 584 (1966).

[3] R. J. Birgeneau, M. T. Hutchings, and W. P. Wolf, Phys. Rev. Letters **17**, 308 (1966).

[4] R. J. Birgeneau, M. T. Hutchings, and W. P. Wolf, J. Appl. Phys. **38**, 957 (1967).

[5] D. P. Landau, R. J. Birgeneau, M. T. Hutchings, and W. P. Wolf, J. Appl. Phys. **39**, 975 (1968).

[6] See for example, A. K. Raychaudhuri and D. K. Ray, Proc. Phys. Soc. (London) **90**, 839 (1967); M. M. Ellis and D. J. Newman, Phys. Letters **21**, 508 (1966); J. Chem. Phys. (to be published).

[7] J. H. Van Vleck, Rev. Mat. Fis. Teor. (Tucuman Argentia) **14**, 189 (1962).

[8] R. Finklestein and A. Mencher, J. Chem. Phys. **21**, 472 (1952).

[9] W. P. Wolf and R. J. Birgeneau, Phys. Rev. (to be published).

[10] K. Sugihara, J. Phys. Soc. Japan **14**, 1231 (1959); L. K. Aminov and B. I. Kochelaev, Zh. Eksperim. i Teor. Fiz. **42**, 1303 (1962) [English transl.: Soviet Phys.—JETP **15**, 903 (1962)]; J. M. Baker and E. A. Mau, Can. J. Phys. **45**, 403 (1967).

cases may prevent the observation of just those transitions which depend most strongly on the interactions.

In this and a following paper, (II), we shall concentrate on interactions involving the simplest of the rare-earth ions, $Gd^{3+}(4f^7)$, for which the orbital effects vanish in the ground state (^8S) so that isotropic exchange and magnetic-dipole interaction may be expected to predominate. We shall show that simple bilinear (Heisenberg) type of exchange together with classical magnetic coupling appropriate to the known lattice spacings do in fact account for the observed spectra to a high degree of accuracy, and that other interactions such as biquadratic or anisotropic exchange are very small, as one might expect. In a subsequent paper (III), we shall describe experiments on Ce^{3+} in $LaCl_3$ which illustrate the highly anisotropic effects which may occur in non-S-state rare-earth ions. In the three papers we shall thus have cause to review all the known interaction mechanisms in rare-earth insulators.

A detailed knowledge of the types and magnitudes of the interactions between Gd^{3+} ions in $LaCl_3$ is of interest not only in connection with the basic understanding of superexchange interactions in rare-earth systems, but also because the isostructural compound $GdCl_3$ is one of the few known ferromagnetic insulators, whose observed cooperative ordering at 2.2°K [11] has not yet been explained. We have therefore made a complete analysis of the EPR spectrum from both nearest-neighbor and next-nearest-neighbor pairs of Gd^{3+} ions isolated in the diamagnetic host lattice. This has enabled us to determine very accurate values for the interaction parameters and to come to quite definite conclusions as regards the ordering of $GdCl_3$, which is shown to arise from a dominant ferromagnetic *next*-nearest neighbor interaction. There is no clear theoretical explanation for such an interaction at this time.

Because of the high relative accuracy inherent in the EPR pair method and the fact that the pair energy levels are almost equally populated even at low temperatures ($T>4$°K), we have been able to extend the measurements to cover a range of temperatures.[3] This has enabled us to determine the interaction parameters, particularly the isotropic exchange, as a function of temperature and we find a small but definite variation. This analysis may be extended by making a few additional assumptions to give the exchange as a function of ionic separations albeit over a small range of values. The results suggest that the interactions appropriate to the $Gd^{3+}-Gd^{3+}$ separation in concentrated $GdCl_3$ may be somewhat different from those measured in $LaCl_3$, and we have therefore carried out a second series of measurements on Gd^{3+} pairs in $EuCl_3$, a host lattice which is effectively nonmagnetic at low temperatures and whose lattice constants are very much closer to $GdCl_3$ than those of $LaCl_3$. These measurements will be discussed in a following paper, (II), and we shall postpone the main discussion of the bulk properties of $GdCl_3$ until then.

[11] W. P. Wolf, M. J. M. Leask, B. Mangum, and A. F. G. Wyatt, J. Phys. Soc. Japan Suppl. **17**, B-1, 487 (1961).

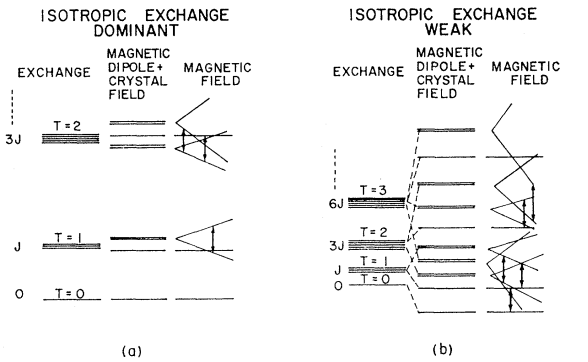

FIG. 1. Energy-level diagram for a pair of antiferromagnetically coupled S-state ions. (a) Exchange dominant, (b) exchange weak compared with magnetic-dipole and crystal-field interactions.

In the present paper we shall explain the principles underlying the pair method for finding weak exchange interactions in S-state ions (Sec. 2) and we shall give the theory of the spectrum which may be expected generally from a pair of $S=\frac{7}{2}$ spins (Sec. 3). The experiments and results will be described in Sec. 4 and interpretation of the spectra will be discussed in Sec. 5. The deduced interaction parameters and their variation with temperature will be discussed in Sec. 6. A summary and general conclusions are given in Sec. 7.

2. PAIR METHOD FOR WEAK INTERACTIONS

The method used in this work is new and differs in some important respects from previous measurements on coupled pairs of S-state ions. In most of the experiments which have been reported so far[12,13] the dominant interaction was a large isotropic exchange coupling, $J\mathbf{S}_1\cdot\mathbf{S}_2$, which leads to an energy-level pattern of the form shown in Fig. 1(a). The corresponding states may be described by a total angular momentum $\mathbf{T}=\mathbf{S}_1+\mathbf{S}_2$, with $|S_1-S_2|\leq T\leq S_1+S_2$ and splittings between the different groups of T states are given by the Landé interval rule. Relatively small additional interactions such as crystal-field or magnetic-dipole terms split the different $(2T+1)$-fold degeneracies, and microwave resonances may be observed between the states belonging to each value of T. Magnetic transitions involving $\Delta T\neq 0$ are forbidden, and the exchange constant J is therefore deduced from the *intensities* of the observed transitions, which are hard to estimate, while the more accurate line positions give information only on the small terms which remove the $(2T+1)$-fold degeneracies.

[12] J. M. Baker and B. Bleaney, in *Proceedings of the International Conference on Low Temperature Physics, Paris, 1955* (Institut International du Froid, Paris, 1955), p. 83.

[13] D. M. A. Bagguley and J. Owen, Rept. Progr. Phys. **20**, 304 (1957); J. H. E. Griffiths, J. Owen, J. G. Park, and M. F. Partridge, Proc. Roy. Soc. (London) **A250**, 84 (1959); J. Owen, J. Appl. Phys. Suppl. **32**, 2135 (1961); **33**, 255 (1962).

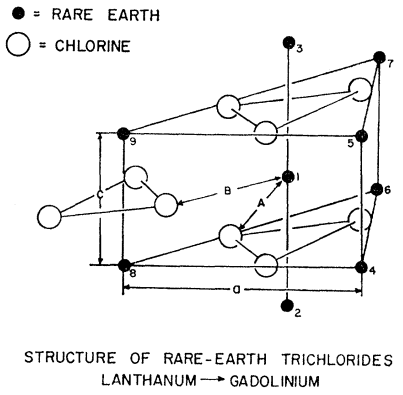

FIG. 2. Crystal structure of the light rare-earth trichlorides. The labeled distances corresponding to $LaCl_3$ and $GdCl_3$ are given in Table I.

A very different situation arises when the exchange is weak and comparable with other nonisotropic interactions. The total angular momentum T is then no longer a good quantum number and transitions between states of predominantly different values of T become allowed. [See Fig. 1(b).] The fields or frequencies at which such transitions occur may then depend on the strength of the isotropic, as well as the anisotropic interactions. Although the spectrum will generally be quite complex, it should now be possible to extract all the interaction parameters from accurately measurable line *positions*, using intensity measurements only as a guide to the identification of the transitions. It should be noted that transitions depending on the isotropic part of the interactions can only be observed if the spin on each ion is greater than $\frac{1}{2}$ or the two spins are inequivalent. One way of obtaining an effective inequivalence is to couple a third spin such as a nuclear spin[12] or that of another ion[14] to one member of the pair. For common S-state ions (Mn^{2+}, Fe^{3+}, Gd^{3+}, etc.) S is always greater than $\frac{1}{2}$ and the only real limitation to the method is the strength of the isotropic exchange relative to the admixing terms, and the available frequencies for observing the transitions.

In practice, pairs of spins are produced by substituting magnetic ions for a small fraction (0.1~10%) of nonmagnetic ones, and depending on the crystal structure and effective range of the interactions, this leads to a number of different types of pairs which will give rise to different overlapping spectra. Also, as the concentration of magnetic ions is increased there is a larger probability of more complex spin clusters, such as triples, which will give additional lines. In order to simplify the identification of the spectra it is necessary therefore to choose an optimum concentration and to make measurements with magnetic fields applied in appropriate crystal directions to pick out the spectra of individual types of pairs. The simple structure of the trichlorides fortunately makes it easy to do this in our case.

The trichlorides from $LaCl_3$ to $GdCl_3$ have the $Y(OH)_3$ hexagonal structure,[15] space group $C6_3/m$ which is shown in Fig. 2. The rare-earth sites are all magnetically equivalent, with point symmetry C_{3h}. The lattice parameters and some related lattice distances for $LaCl_3$ and $GdCl_3$ are given in Table I. From Fig. 2 we may see that any given cation site (1) has two equivalent nearest neighbors (nn) (2 and 3) and six next-nearest neighbors (nnn) (4 to 9), slightly further away, while the 3rd nearest neighbors are almost twice as far. In considering the types of pair spectra which will be resolved from the single-ion lines it is reasonable therefore to neglect the effects of third and more distant neighbors and to concentrate on nn and nnn pairs. We shall show that this is consistent with our observations.

Assuming a random occupation of the cation sites with magnetic ions at a concentration c, the probability of finding a nn pair which has no other magnetic spins in either nn or nnn positions is $c^2(1-c)^{11}$, while the probability of an isolated nnn pair is $3c^2(1-c)^{12}$. The corresponding factors for a pair with one or more additional nearest or next-nearest neighbors are $c^2[1-(1-c)^{11}]$ and $3c^2[1-(1-c)^{12}]$ and we can see therefore that simple pair spectra will be obtained only if c is relatively small. On the other hand, the over-all intensity also decreases rapidly with c and it is therefore necessary to strike a compromise. In practice concentrations near $c=0.01$ were found to be satisfactory.

Even with only nn- and nnn-type pairs there are still seven different spectra for a magnetic field applied in an arbitrary direction, but we may use the fact that for the Hamiltonian expected in our case the lines in each pair spectrum have turning values as the field direction is varied close to the particular pair axis. (See Sec. 4.) The samples were therefore oriented with a plane containing the c axis and one of the nnn pair axes parallel to the horizontal plane in which the magnetic field could be swept. In practice the resolution of the two types of spectra proved to be particularly simple in our case because the angle between the two axes (63.2°) is close to the angle at which $3\cos^2\theta-1=0$, with the result that the first-order effect of the magnetic-dipole interaction for one type was very small when the other was at its

TABLE I. Lattice constants in $LaCl_3$ and $GdCl_3$ (Å).

	$c(\equiv r_{nn})$	a	r_{nnn}	A	B
$LaCl_3$	4.375[a]	7.483[a]	4.843	2.91[b]	2.96[b]
$GdCl_3$	4.105[a]	7.363[a]	4.721	2.82[b]	2.91[b]

[a] See Ref. 15 and D. H. Templeton and C. H. Dauben, J. Am. Chem. Soc. 76, 5237 (1954); and C. Au and R. Au, Acta Cryst., 23, 1112 (1967).
[b] The rare-earth–chlorine distances A and B depend on two parameters x and y which have only been determined for the cases of $GdCl_3$ and isostructural UCl_3, but the variation is small and we may take the $GdCl_3$ values for $LaCl_3$ and the other rare-earth chlorides.

[14] E. A. Harris and J. Owen, Proc. Roy. Soc. (London) A289, 122 (1965).

[15] W. H. Zachariasen, J. Chem. Phys. 16, 254 (1948).

maximum, and vice versa. With other crystal structures such a simplification will generally not occur, but the characteristic angular variations of the different spectra will usually make it possible to classify the observed lines.

3. THEORETICAL SPECTRUM OF A PAIR OF $S=\frac{7}{2}$ IONS

Before describing the experimental results we shall discuss the theory of the types of spectra we may expect from a pair of interacting Gd^{3+} ions, and in particular we shall consider a truncated form of the complete Hamiltonian which will be a good first approximation for both the nn and nnn spectra in our case, and also in most other systems involving pairs of $S=\frac{7}{2}$ spins. We shall defer the discussion of various small terms which may be required to obtain a complete fit to the observed spectra until Sec. 5, in which we shall also estimate the approximate values of the various parameters which we may expect in our case.

A. General Pair Hamiltonian

Taking the pair axis as the z direction and assuming the magnetic g factors to be isotropic, the general pair Hamiltonian may be written as

$$\begin{aligned}\mathcal{H}(1,2)=&J\mathbf{S}_1\cdot\mathbf{S}_2+(g^2\mu_B^2/r^3)(\mathbf{S}_1\cdot\mathbf{S}_2-3S_{z1}S_{z2})\\&+g\mu_BH_z(S_{z1}+S_{z2})\\&+g\mu_BH_x(S_{x1}+S_{x2})+V_c+\mathcal{H}_{\rm int}{}^{(1)},\end{aligned}\quad(1)$$

where the first two terms represent the isotropic exchange and magnetic-dipole interactions, the next two the Zeeman terms for fields parallel and perpendicular to the pair axis (μ_B is taken as a positive number), V_c the crystal field and $\mathcal{H}_{\rm int}{}^{(1)}$ higher-order interaction effects, such as anisotropic or antisymmetric superexchange, biquadratic exchange or magneto-elastic effects. For a rare-earth S-state ion such as Gd^{3+} we would expect all the terms in $\mathcal{H}_{\rm int}{}^{(1)}$ to be extremely small and we shall only consider them in Sec. 5 C in connection with some very small discrepancies in the final fit. The crystal-field terms will generally also be quite small, and we may pick out their most important contribution in the usual way by defining them relative to the same axis of quantization as the large terms in $\mathcal{H}(1,2)$, (here the pair axis), retaining only the diagonal terms ($V_c{}^{(0)}$). The remaining off-diagonal terms $V_c{}^{(1)}$ will produce small line shifts in second order, but these may effectively be eliminated by averaging corresponding low- and high-field transitions. Correct to second order we may therefore represent the crystal field by an operator of the form

$$\begin{aligned}V_c{}^{(0)}=&\textstyle\sum_{i=1,2}(1/3)b_2{}^0O_2{}^0(i)+(1/60)b_4{}^0O_4{}^0(i)\\&+(1/1260)b_6{}^0O_6{}^0(i),\end{aligned}\quad(2)$$

where the $O_n{}^0$ are the standard crystal-field operators,[16] and the $b_n{}^0$ are *effective* parameters defined relative to each pair axis.

We may similarly simplify the Zeeman terms by omitting the off-diagonal x components. Physically this corresponds to restricting the magnetic field to directions close to the particular pair axis and treating any small deviations by second-order perturbation theory (see Sec. 3E).

Correct to first order our general pair Hamiltonian may thus be written in the form

$$\mathcal{H}^{(0)}(1,2)=\mathcal{H}_{\rm int}{}^{(0)}+\mathcal{H}_z{}^{(0)}+V_c{}^{(0)},\quad(3)$$

where

$$\begin{aligned}\mathcal{H}_{\rm int}{}^{(0)}+\mathcal{H}_z{}^{(0)}=\mathcal{H}_p{}^{(0)}=&J\mathbf{S}_1\cdot\mathbf{S}_2+\alpha(\mathbf{S}_1\cdot\mathbf{S}_2-3S_{z1}S_{z2})\\&+g\mu_BH_z(S_{z1}+S_{z2}),\end{aligned}\quad(4)$$

$\alpha=g^2\mu_B{}^2/r^3$ and $V_c{}^{(0)}$ is given in Eq. (2).

B. Zero-Order Pair Hamiltonian

Neglecting for the moment $V_c{}^{(0)}$ and any transverse Zeeman terms we are left with three nontrivial terms in Eq. (4) which should dominate the form of the pair spectra in appropriate cases. However, even with this simplification it is still not trivial to find the energy levels since there is no convenient near-diagonal representation unless α is negligible, which is not the case when the exchange is also weak. One must therefore treat the problem numerically using the symmetry of $\mathcal{H}_p{}^{(0)}$ first to eliminate all redundant calculations. As basis states we may either use $|S_1,S_2,M_1,M_2\rangle$ or $|S_1,S_2,T,M\rangle$ where $\mathbf{T}=\mathbf{S}_1+\mathbf{S}_2$. The situation is clearer physically when discussed in terms of the latter representation but the former is more convenient for writing down the energy matrix as the first step in the numerical diagonalization. In either case we start with a 64×64 matrix which fortunately can be factorized into 15 smaller matrices each characterized by basis states having the same value of $M=M_1+M_2$ and of dimension $8-|M|$. Furthermore, since the operators in $\mathcal{H}_p{}^{(0)}$ admix only states with $\Delta T=2$, we can subdivide the secular determinants further into those characterized by basis states which are admixtures of either odd- or even-T states. Finally, as the Zeeman term $g\mu_BH_zT_z$ is a constant diagonal term within each submatrix it may be factorized out and considered separately. This enables us to calculate exact resonance fields directly from the zero-field energy levels and provides an important simplification. The problem of predicting the pair spectrum corresponding to $\mathcal{H}_p{}^{(0)}$ is thus reduced to diagonalizing four 2×2, four 3×3 and three distinct 4×4 determinants. These calculations are readily carried out using a digital computer, for which we used the Yale IBM 7040-7094.

In practice, the matrices were compiled in the $|S_1,S_2,M_1,M_2\rangle$ representation in which the single-ion crystal-field terms may also be included most conveniently. They were then transformed to a $|S_1,S_2,T,M\rangle$ representation by the use of the appropriate Clebsch-

[16] See for example, M. T. Hutchings, in *Solid State Physics*, edited by F. Seitz and D. Turnbull (Academic Press Inc., New York, 1964), Vol. 16, p. 227.

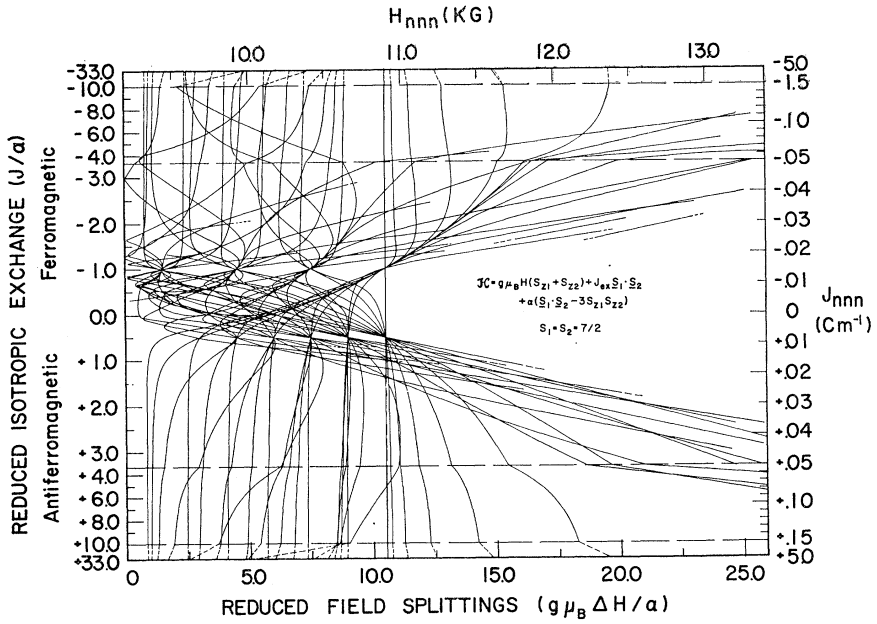

FIG. 3. Theoretical EPR spectra for pairs of coupled $S=\frac{7}{2}$ S-state ions with exchange constant J, dipolar constant $\alpha=g^2\mu_B^2/r^3$ and the magnetic field applied along the pair axis. The lower and left-hand scales give the reduced field splittings, $g\mu_B\Delta H/\alpha$, as a function of reduced exchange J/α. The upper and right-hand scales give the high-field spectrum for the case $g=1.9915$, $\alpha=0.01511$ cm^{-1}, $\nu=25.625$ GHz. The lines plotted are those with intensities above about 1/50 of that of the strongest resonance assuming equal population of all the pair levels.

Gordan coefficients. After factorization into odd- and even-T matrices, they were diagonalized to give eigenvalues and eigenvectors of the form

$$E=g\mu_B H_z M+E(|M|,k)$$

and

$$|M,k\rangle=\sum_{\text{(odd or even } T)} a_T|S_1,S_2,T,M\rangle,$$

where k is an integer index which distinguishes different states of the same value of M.

The resonance fields for transitions with $\Delta T=0$, $\Delta M=\pm 1$ could then be calculated in a straightforward manner from

$$g\mu_B H_z=h\nu\pm[E(|M+1|,k)-E(|M|,k')]. \quad (5)$$

If we assume that the relative intensities are governed primarily by magnetic-dipole transition probabilities, they may readily be estimated from

$$I\approx\text{const}\times|\langle M,k'|T_x|M+1,k\rangle|^2, \quad (6)$$

using the zero-field eigenfunctions.

We would therefore expect pairs of equally intense lines to occur symmetrically about the center of the single-ion spectrum $H_0=h\nu/g\mu_B$, with splittings independent of frequency. These are two very important criteria in identifying the spectra and confirming the adequacy of $\mathcal{H}_p^{(0)}$. As the splittings from the center are independent of frequency the spectra can be characterized by just two variables, the ratios α/g and J/α, and in Fig. 3 we show the variation of reduced splittings $|g\mu_B H/\alpha|$ as a function of J/α. If g and α can be estimated from the single-ion resonance and the crystal structure, this figure can be rescaled to show actual resonance fields at a given frequency ν for different values of the exchange parameter J. The upper- and right-hand scales in Fig. 3 illustrate the case $g=1.9915$, $\alpha=0.01511$ cm^{-1}, $\nu=25.625$ GHz corresponding to values close to those appropriate to nnn Gd^{3+} pairs in $LaCl_3$, and the frequency used in most of our experiments. The lines shown in this figure are those whose intensities are predicted to be observable with our spectrometer (about 46 lines in each half of the spectrum) out of a total of 84 lines allowed by the selection rules. In general the intensities decrease as the splittings from the center increase, but they also vary with J/α and we shall therefore defer discussions of the intensity predictions until we consider the detailed comparison between the predicted and observed spectra (Secs. 5 C and 5 D).

Figure 3 shows several interesting features. As we would expect on the basis of the general discussion in Sec. 2, the line positions become relatively insensitive to J when $|J|\gg|\alpha|$, (note the changes of scale at the broken lines), corresponding to the situation encountered in most previous pair studies. On the other hand for cases of weak exchange interactions, ($|J|<\sim 3|\alpha|$), some lines depend quite strongly on J and a fit to the spectrum can then give an accurate measure of the exchange interaction. The lines most sensitive to J are generally those which are forbidden in the large-J limit, that is those between states with predominantly different T, which only become admixed when the anisotropic terms become comparable with the isotropic terms ($\alpha\sim J$).

For two special values of J/α (-1 and $+\frac{1}{2}$) large numbers of the transitions coalesce into a small number of highly degenerate lines, as may be seen in Fig. 3.

(1) When $J=-\alpha$ there are only four equally spaced lines in each half of the spectrum. This is because for this value of J, the interactions reduce to $-3\alpha S_{z1}S_{z2}$,

corresponding to an Ising-type coupling, and the four transition fields correspond to one of the spins flipping while the other is in the $M_2=\frac{7}{2}, \frac{5}{2}, \frac{3}{2}$, or $\frac{1}{2}$ state.

(2) When $J=\frac{1}{2}\alpha$ the high- and low-field transitions each coalesce into seven equispaced lines. This somewhat surprising degeneracy arises because for this value of J the interactions reduce to

$$\mathcal{H}=J'[S_{z1}S_{z2}-(S_{x1}S_{x2}+S_{y1}S_{y2})],$$

with $J'=-3J$, which we would expect to give the same energy levels as $\mathcal{H}'=J'\mathbf{S}_1\cdot\mathbf{S}_2$, since $\mathcal{H}$ and $\mathcal{H}'$ are related by a 180° rotation of the coordinates of spin 1 about the z axis. We might therefore expect the same transitions as in the corresponding high-J limit (i.e., no transitions between different T multiplets), but in fact $\mathcal{H}$ and $\mathcal{H}'$ have basically different eigenvectors and those of $\mathcal{H}$ are just such as to allow strong transitions between levels belonging to the different T multiplets of $\mathcal{H}'$, and thus give the seven lines. However, in practice a very much larger number of lines will generally be observed even in these two high-degeneracy regions because of splittings and shifts produced by the small terms we have neglected so far. We therefore consider two of these next.

C. Effect of Small Crystal-Field Terms

As discussed above, it is generally a very good approximation to consider only those crystal-field terms which are diagonal with respect to the pair axis as axis of quantization, as in Eq. (2), and such terms are readily added to the energy matrix in its $|M_1M_2\rangle$ representation. The extra terms do not affect the factorization of the matrix and, most important, they do not destroy the symmetry of the spectrum about its center. If the parameters b_n^0 are small, as they are in the case of Gd^{3+} in $LaCl_3$ (see Sec. 5A), their principal effect is to shift the lines by small amounts (~100 G) in a systematic way. This can easily be studied by adding different combinations of crystal-field terms to $\mathcal{H}_p^{(0)}$ in the computer program which leads to Fig. 3. Once the different lines in the observed spectrum have been identified with specific transitions all three b_n^0 can be included simultaneously and fitted together with the parameters J, α, and g. In less favorable cases it may be necessary to include one or more of the b_n^0 to obtain a definite identification (see for example II), but for a preliminary analysis of the spectrum, Fig. 3 without any b_n^0 terms generally serves as an excellent guide.

D. Angular Variation

The angular variation as the direction of the field is varied close to the pair axis is an important guide in the identification of the spectra. So far we have neglected the transverse Zeeman terms, $g\mu_B H_x(S_{x1}+S_{x2})$, as they destroy the simplifiying factorization of the energy matrix, and an exact treatment would involve the diagonalization of large 64×64 matrices. However in the neighborhood of the pair-axis, perturbation theory will give the resonance fields to sufficient accuracy.

If a magnetic field H is applied at an angle θ to the pair axis we may take the zeroth-order Hamiltonian as Eq. (3) and the perturbation Hamiltonian as

$$\mathcal{H}'(\theta)=g\mu_B H(\cos\theta-1)T_z+g\mu_B H\sin\theta T_x. \quad (7)$$

It is then a straightforward application of first- and second-order perturbation theory to show that the change in the resonance field for the transition $|m\rangle\rightarrow|n\rangle$ as a function of angle is given by

$$\Delta H_{mn}=\epsilon_{mn}(1-\cos\theta/\cos\theta)H+(\sin^2\theta/\cos\theta)B_{mn}, \quad (8)$$

where

$$B_{mn}=g\mu_B H^2(Q_m-Q_n)$$

with

$$Q_m=\sum_{l\neq m}\frac{|\langle m|T_x|l\rangle|^2}{E_m-E_l}$$

and

$$E_m-E_l=E_m(H=0)-E_l(H=0)-\epsilon_{lm}g\mu_B H.$$

Here $|l\rangle$, $|m\rangle$, and $|n\rangle$ denote eigenvectors of $\mathcal{H}^0(1,2)$ in Eq. (3), with $M=M(l)$, $M(m)$, and $M(n)$, respectively, and $\epsilon_{lm}=M(l)-M(m)=\pm1$.

Calculations of the resonance line shifts for different values of θ were carried out on a computer, using Eq. (8), and the results will be discussed in conjunction with the fitting of the spectrum. In order to check the validity of these perturbation calculations, a program was written to diagonalize the complete 64×64 matrix for an arbitrary field and angle, and the resonance fields for several transitions were calculated exactly and compared with the perturbation results. In general it was found that out to 20° from the pair axis the perturbation theory predicted the shifts to about 5% (±10 G). Occasionally it was found that due to accidental near degeneracies the perturbation theory broke down, but these were easily detected and the true angular variation could then be calculated using the 64×64 matrix diagonalization program.

We may note that the change in resonance field ΔH_{mn} is independent of the sign of θ and therefore the pair lines should turn symmetrically about the pair axis. As we shall see this forms a good test of the validity of the Hamiltonian used, and together with the symmetry of the spectrum about its center and the frequency dependence, it forms a check on the size of any off-diagonal terms not included in $\mathcal{H}^{(0)}(1,2)$.

4. EXPERIMENTAL RESULTS

A. Samples and Apparatus

Single crystals were grown from mixed powders of the anhydrous trichlorides by G. Garton and S. Itzkowitz at Oxford and S. Mroczkowski at Yale using the Bridgeman-Stockbarger method in a manner similar to that

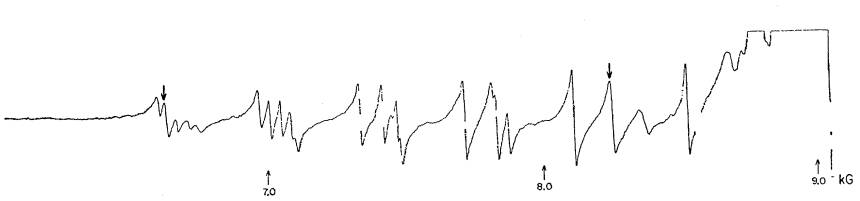

FIG. 4. Low-field half of nearest-neighbor pair spectrum at $T=77°K$ and $\nu=25.625$ GHz with the magnetic field along the c axis.

described by Garton *et al.*[17] Gd^{3+} concentrations close to 1% were generally used and most samples contained, in addition, 1% of Ce^{3+} to shorten relaxation times at low temperatures. The crystals were oriented using the Laue method of back reflection of x rays. Most of the samples were oriented so that the plane containing the c axis and an nnn bond axis was horizontal, enabling the magnetic field to be swept in this plane. This was accomplished by ensuring that one of the three more intense lines of spots on the photograph was horizontal.[18] On inspection by EPR the samples were often found to be twinned and only samples which showed untwinned spectra were used. A minor disadvantage of the rare-earth trichlorides is that they are hygroscopic, but the rate of hydration is sufficiently slow that this difficulty could be easily overcome. In general the crystals were stored in dried paraffin oil and handled in a dry box, and when the crystals had to be exposed to air, as during orientation, a thin layer of Apiezon N grease was found to be quite adequate to protect them.

Measurements were made at both X band (9.51 GHz) and K band (25.6 GHz) frequencies using transmission spectrometers of conventional design,[19] incorporating 115 kcycle/sec field modulation and phase-sensitive detection. The magnetic field was provided by a Varian 12-in. "Field dial" system and measured with a "Numar" NMR gaussmeter and Hewlett Packard frequency counter. The field could be modulated at 60 Hz for oscilloscope display or swept at adjustable speeds for chart display. The microwave frequency was measured at X band with a transfer oscillator, and at K band with a calibrated wave meter.

Temperatures in the range 1.6–300°K were obtained by using different liquid refrigerants. Experiments were performed using helium (1.6–4.2°K), hydrogen (20°K), nitrogen (77°K), CF_4 (145°K), CO_2 and acetone (195°K), $CHClF_2$ (232°K), CCl_2F_2 (243°K) and ice and water (273°K). For higher temperatures paraffin oil heated electrically up to 90°C was used.

TABLE II. Single-ion crystal-field parameters for Gd^{3+} in $LaCl_3$.

Temp. (°K)	290[a]	90[a]	20[b]
g	1.991	1.991(±0.001)	1.9915(±0.0006)
b_2^0 (10^{-4} cm^{-1})	8.36(±0.10)	16.0(±0.20)	18.0(±0.2)
b_4^0 (10^{-4} cm^{-1})	1.68(±0.04)	2.13(±0.05)	2.14(±0.05)
b_6^0 (10^{-4} cm^{-1})	0.64(±0.15)	0.25(±0.05)	0.23(±0.05)
b_6^6 (10^{-4} cm^{-1})	···	1.40(±0.3)	0.13(±0.07)

[a] Reference 20.
[b] Reference 19.

B. Single-Ion Spectrum

Before discussing the pair lines observed we shall briefly refer to the resonance from single ions of Gd^{3+} in $LaCl_3$. This was first observed by Hutchison *et al.*,[20] and their results are given in Table II together with some later measurements. The symmetry at the rare-earth site is C_{3h} and there are four spin-Hamiltonian parameters describing the crystal-field interaction, b_2^0, b_4^0, b_6^0, and b_6^6 (if the axes are chosen appropriately). The most noticable feature is that the values of b_n^m are small, the over-all spread of the spectrum being only 300 G and 90°K. It seems reasonable to assume that for a pair of ions the values of b_n^0 will remain small, and this was our reason for their neglect in the initial discussion of Sec. 3B. The hyperfine interaction is very small and only broadens the lines slightly without giving rise to any satellite lines.

C. Nearest-Neighbor Pair Spectrum

1. *Spectrum with the Magnetic Field along the c Axis*

In addition to the seven single-ion Gd^{3+} transitions, the EPR spectrum with $\mathbf{H}\|c$ axis was found to contain a large number of weaker lines symmetrical about the center and extending out to about ±2600 G. The low-field half of this spectrum at 77°K, $\nu=25.625$ GHz is shown in Fig. 4. At the right of the figure, well beyond the full-scale deflection of the chart recorder, are the single-ion lines. From the figure it may be seen that most of the pair lines occur in groups about 140 G wide separated by about 370 G. When the magnetic-field angle was varied it was found that nearly all of the lines with splittings greater than 680 G turned symmetrically about the c axis, suggesting strongly that they are all due to nn pairs, and that the lines due to other pairs are close to the center, as we expect. The one line just to the right of the arrow at about 8.3 kG in Fig. 4 is in

[17] G. Garton, M. T. Hutchings, R. Shore, and W. P. Wolf, J. Chem. Phys. **41**, 1970 (1964).
[18] R. J. Birgeneau, thesis, Yale University, 1966 (unpublished).
[19] M. T. Hutchings, thesis, Oxford University, 1963 (unpublished).
[20] C. A. Hutchison, B. R. Judd, and D. F. D. Pope, Proc. Phys. Soc. (London) **B70**, 514 (1957).

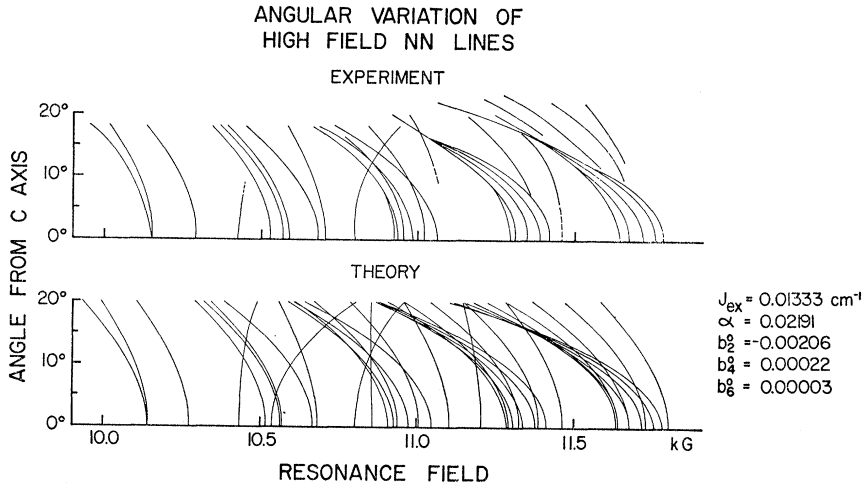

FIG. 5. Experimental and calculated angular variations of the high-field nearest-neighbor pair transitions at $T=77°K$ and $\nu=25.625$ GHz. There is a slight relative shift of the whole spectrum due to a small difference in the frequencies of measurement and calculation. The center of the spectrum is at 9.193 kG corresponding to $g=1.9915$.

fact a crossing and has no high-field counterpart, and is therefore probably due to another type of pair or else an impurity. Measurements of line positions were made using both chart and scope displays of the absorption derivatives and the average of these readings at X- and K-band frequencies are given in Table III. Linewidths were generally 10–20 G and if well resolved the line positions could be measured to an accuracy of about ± 4 G. From the table it may be seen that the pair lines at both X and K band are all symmetrical about the central single-ion transition (given by $H_0=h\nu/g\mu_B$), and that the splittings at the two frequencies agree with each other to within the experimental error. These two striking features are predicted by the truncated Hamiltonian $\mathcal{H}^0(1,2)=\mathcal{H}^0+V_c^{(0)}$, and they show that any terms which may have been omitted from Eq. (3) must either be very small or have a specially simple form which preserves the symmetry and frequency independence.

The intensities of the observed pair transitions were found to vary by a factor of about 100, as estimated from the peak-to-peak heights of the absorption derivatives, and they will be compared with the theoretical predictions in Sec. 5 C. A careful search for other lines, especially at higher fields, showed that there are no lines with splittings greater than 2600 G with intensities greater than 1/20 of the weakest line listed in Table III, except for one group of four extremely weak lines symmetrically placed about the center at ± 3900 G. As we shall see later the absence of lines with large splittings is in accord with the final fit to the observed spectrum which predicts only very weak transitions beyond ± 2600 G. Perhaps the most likely origin of the weak group at ± 3900 G is a cluster of three interacting ions, but in any case we conclude that they are almost certainly not due to nn pairs.

In both the nn and nnn spectra a number of weak subsidiary lines were also observed centered about a field which was exactly half that of the central single-ion resonance. Such weak "half-field" lines can arise from various off-diagonal crystal field or interaction terms, produced by asymmetrically placed neighboring ions, which admix the single-ion states slightly and make $\Delta M=2$ transitions possible.[21] Such lines have no counterparts at high fields and are readily distinguished from the true $\Delta T_z=1$ transitions of nn pairs.

In summary, the nn spectrum is composed of about 50 lines, symmetric about H_0 with splittings indepen-

TABLE III. Relative fields (in gauss) of nn pair lines with respect to the central transition at 77°K and at 25.6 and 9.5 GHz. The error is generally ± 4 G for the K band, ± 5 G for the X band measurements. The central transition corresponds to a g value of 1.9915.

K band 25.6 GHz		X band 9.5 GHz	
ΔH_-	ΔH_+	ΔH_-	ΔH_+
−2591.2	2589.5	−2591	2590
−2563.0	2562.3	−2560	2564
−2522.7	2521.3	−2527	2523
−2477.9	2478.2	−2479	2484
−2445.9	2444.1	−2454	2447
−2224.4	2223.7	−2223	2217
−2187.9	2186.8	−2188	2188
−2147.1	2146.4	−2146	2145
−2111.8	2110.2	−2104	2108
−2094.4	2093.0	−2093	2096
−1862.9	1861.9	−1858	1860
−1782.5	1780.9	−1781	1779
−1752.5	1751.2	−1753	1752
−1733.6	1731.9	−1733	1732
−1721.0	1719.0	−1724	1719
−1482.5	1482.8	−1479	1480
−1383.6	1382.8	−1382	1388
−1370.2	1369.0	−1365	1374
−1326.9	1326.9	−1332	1329
−1087.4	1087.6	−1085	1085
−947.4	947.4	−948	949
−678.3	679.1	−678	678

[21] See for example, H. A. Buckmaster, in *Proceedings of the First International Conference on Paramagnetic Resonance* (Academic Press Inc., New York, 1963), Vol. 1, p. 217.

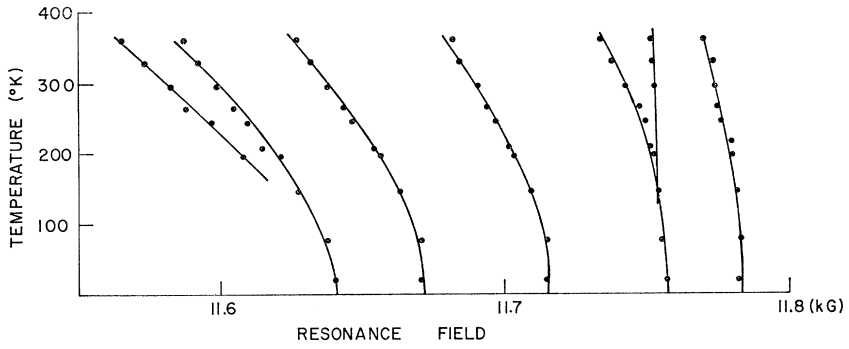

FIG. 6. Temperature variation of the resonance fields of the outer group of nearest-neighbor pair lines with the magnetic field along the c axis.

dent of frequency. The spectrum subdivides into four well-resolved outer groups of lines with three inner well-resolved lines, and there are no lines further than ± 2600 G from the center of the spectrum.

2. *Angular Variation*

The angular variation of the nn lines out to 20° from the c axis was studied at K band for both high and low fields. The resonance fields were found to be accurately symmetrical about the c axis, as required by the axial symmetry. The results for the high-field nn transitions are given as the experimental part in Fig. 5. The calculated angular variation in Fig. 5 will be discussed in Sec. 5 C. The angular variation demonstrates the presence of several smaller unresolved lines within the groups which emerge off axis; also two lines marked with arrows in Fig. 4 are seen to split off-axis and both in fact are two coincident lines. The two outermost groups each coalesce into a single broad line at about 15° off-axis, due to a substantially different angular variations of the different inner lines.

3. *Temperature Variation*

So far we have only discussed the experimental results obtained at 77°K, which are in fact almost identical to those found at lower temperatures. However, as the temperature is raised and thermal expansion becomes appreciable the spectra begin to show marked changes, which we can interpret in terms of a temperature dependence of the parameters in $\mathcal{H}(1,2)$. The measurements at different temperatures also provide an excellent indication of the consistency of the results since we would expect the line positions to vary smoothly as the parameters change. Figure 6 shows the variation of the splittings of the outer group of nn pair lines from 20 to 361°K. As the temperature was increased the line widths also increased, reaching 20–30 G at 361°K, but since the splittings between the lines also tended to increase the over-all resolution remained roughly constant. These and similar results for other lines confirm the accuracy of the measurements (± 4 G) and, as will be shown in Sec. 6B, they indicate a significant variation of the exchange and dipole interactions.

D. Next-Nearest-Neighbor Pair Spectrum

1. *Spectrum with the Magnetic Field along the nnn Axis*

When the direction of the magnetic field was varied away from the c axis a series of lines were found to turn about an angle of 63.2° (± 0.5). Since this is within the experimental error equal to the angle the nnn bond axis makes with the c axis these lines were attributed to next-nearest neighbor pairs. The low-field half of the EPR spectrum at 77°K, $\nu = 25.625$ GHz, with the magnetic field at 63.2° to the c axis is shown in Fig. 7. As in the nn case, the spectrum is composed of large single-ion lines (well off full-scale deflection on the chart recorder in Fig. 7), with a number of smaller lines on either side extending out to about ± 3900 G from the central transition. All of the larger pair lines and most of the smaller lines with splittings greater than 1000 G were found to be symmetrical about the central single-ion transition within experimental error. However, at splittings less than 1000 G there were a number of large lines which were definitely not symmetrical about the center. On varying the angle of the magnetic field it was found

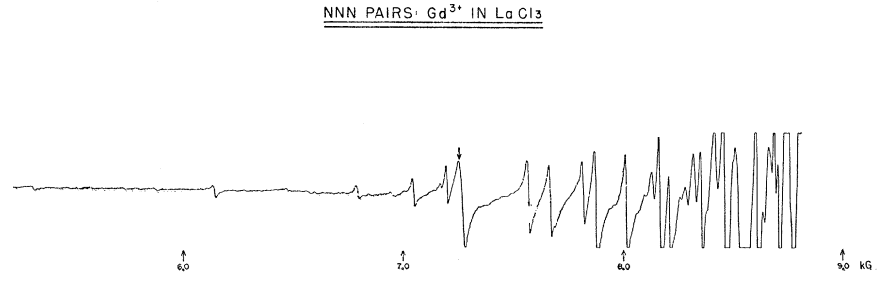

FIG. 7. Low-field half of next-nearest neighbor pair spectrum at $T = 77$°K and $\nu = 25.625$ GHz with the magnetic field along the nnn bond axis.

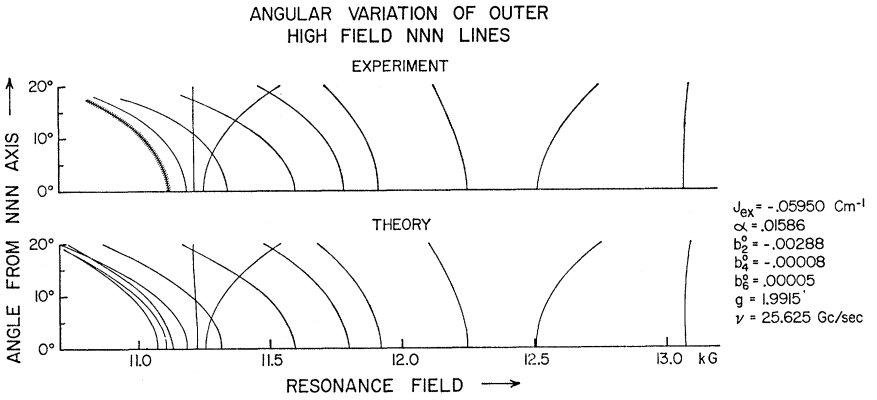

FIG. 8. Experimental and calculated angular variation of the high-field next-nearest neighbor pair transitions at $T=77°K$ and $\nu=25.625$ GHz. The center of the spectrum is at 9.193 kG.

that all of the lines which were symmetrical about the center also had turning values at 63.2 ($\pm 0.5°$), while most of the other lines were quite asymmetric in their angular variation and in fact often split into several lines. Thus, as in the case of the nn pairs, there was no difficulty in separating out the pair transitions. This again was possible because of the somewhat fortuitous fact that the nn and nnn axes are at about 60° to each other.

From Fig. 7 it may be seen that the nnn spectrum extends over a much wider range of fields than the nn spectrum, despite the fact that the dipolar interaction is smaller, and there are no obvious features such as the grouping observed for the nn. The lines tended to decrease in intensity with an increase in field splitting from the center of the spectrum, with the exception of the line marked with an arrow in Fig. 7. On determining the angular variation, this line was found to split into three when **H** lay off the nnn axis, although the splitting was very small. The average line positions of the nnn lines at X band and K band at 77°K are given in Table IV. The fields are the mean of readings taken on both chart and scope displays which were generally consistent to better than ± 4 G. The lines omitted from the table at X band were weak transitions which could only be detected at K band. To check the accuracy of alignment, which is critical for this spectrum, a second crystal was oriented in the same manner and found to give identical resonance fields within the estimated accuracy.

From Table IV we see that within experimental error all of the transitions at K band are symmetrical about the center and in most cases are in agreement with the X-band results, as for the nn pairs. There are, however, a few irregularities at X band which on fitting the spectrum were found to be due to level crossings. These will be discussed in Sec. 5D.

2. *Angular Variation*

The angular variation of the nnn transitions at K band was studied for both the high- and low-field lines out to 20° on either side of the nnn pair axis. The resonance fields were found to be symmetrical about the pair axis to within about 10% of the deviation from the field along the axis. This is a somewhat surprising result since it indicates that the crystal-field symmetry is predominantly axial about the pair axis rather than the single-ion point symmetry axis. The results of the measurements for the outer high-field lines are shown in Fig. 8, from which it may be seen that most of the lines have quite individual angular variations. This provided a very strong check on the final fit and was a very useful aid for identifying the transitions. The low-field outer transitions have equally characteristic angular variations, quite different, of course, from the corresponding ones at high field.

TABLE IV. Relative fields (in gauss) of nnn pair lines with respect to the central transition at 77°K and at 25.6 and 9.5 GHz. The error is generally ± 4 G for the K band and ± 6 G for the X band measurements. The central transition corresponds to a g value of 1.9915.

K band (25.6 GHz)		X band (9.5 GHz)	
ΔH_-	ΔH_+	ΔH_-	ΔH_+
−3885	3879		
−3322	3323		
−3055.1	3057.3	−3057	3056
−2722	2718		
−2592	2591		
−2406.9	2401.7		
−2150.9	2149.6	−2159.4	2162.6
−2054	2059	−2045.1	2040.4
−2021.7	2024.8		
−1994.0	1991.2	−1991.0	1993.2
−1926.8	1923.8	{−1929.3, −1915.7}	{1934.4, 1912.0}
−1628.5	1627.9	−1626.2	1628.5
−1531.1	1530.4	−1524.8	1524.9
−1384.3	1380.8	−1380.6	
−1327.7	1327.3	−1326.0	
−1181.6	1180.0	−1180.3	−1176.1
−1134	1130		
−1062.5	1061.2	−1067.2	1065.0
−1029.9	1028.1	−1027.5	1050.6
−988.1	986.5	−983.7	998.3
−840.8	839.0	−839.7	833.2
−775.3	775.6	−792.6	792.1
−733.2	732.4	−734.3	748.1

TABLE V. Exchange constants in $GdCl_3$.[a]

A	*B*
$J_{nn}=-0.098\pm0.007$ cm^{-1}	$J_{nn}=+0.028\pm0.015$ cm^{-1}
$J_{nnn}=-0.015\pm0.007$ cm^{-1}	$J_{nnn}=-0.057\pm0.003$ cm^{-1}

[a] After Ref. 22.

3. *Temperature Variation*

One very striking feature of the nnn spectrum is its maked temperature variation. Several of the small outer lines shifted by as much as 500 G between 77°K and room temperature and most of the more intense inner lines shifted by at least 50 G. For most of the lines the splittings from the center were found to decrease with increasing temperature, but for one of the inner lines (1,12) the splitting actually *increased* by over 100 G. This behavior is generally consistent with the variation expected from Fig. 3 assuming that J, α, and J/α decrease as T increases, and provides an extremely valuable check on the identifications made. A quantitative check is provided by the final sets of interaction parameters fitted to the spectra at different temperatures, which show smooth monotonic trends, as we would expect.

E. More Distant Neighbors

A sample oriented so that the magnetic field could be swept through the 3rd nn bond axis was also investigated. However, because there is no fortuitous closing in of the unwanted pair lines, as in the case of the nn and nnn, only a few distinct 3rd nn pair transitions could be observed. These were distinguished by their turning points with the field perpendicular to the c axis. It was concluded that even with known nn and nnn pair line positions the spectrum was so dense in lines that it would be very difficult indeed to obtain information on the 3rd nn interaction, particularly as most of the lines are expected to be at small splittings ($\Delta H<360$ G) from the central transitions, corresponding to $J\approx0$ and $\alpha\sim0.2\alpha_{nn}$.

All the more distant neighbors will similarly give rise to lines which are all close to the center, H_0. We conclude therefore that lines from more distant neighbor pairs will not be resolved in the trichloride lattice, unless they were to be coupled by some more unexpected long range anisotropic nondipolar interaction.

5. INTERPRETATION OF THE SPECTRA

In Sec. 3 we discussed a truncated form of the total spin Hamiltonian of a pair, involving only terms with axial symmetry about the pair axis, and we shall now show that this provides an excellent approximation for the description of both nn and nnn Gd^{3+} pair spectra in $LaCl_3$. The Hamiltonian $\mathcal{H}^{(0)}(1,2)=\mathcal{H}_p{}^{(0)}+V_c{}^{(0)}$ [Eq. (3)] contains six parameters and we shall first attempt to estimate these from previously available data to provide a starting point for the detailed fitting of the observed spectra. The fitting procedure and results will then be described, and finally we consider some of the effects which could account for the small residual discrepancies which cannot be explained using $\mathcal{H}^{(0)}(1,2)$ alone.

A. Approximate Values of the Parameters in $\mathcal{H}^{(0)}(1,2)$

1. *Zeeman Terms*

The magnetic g value has been measured for single Gd^{3+} in $LaCl_3$ and found to be isotropic and equal to 1.991,[20] and we would expect to find a very similar value for the pairs.

2. *Isotropic Exchange*

Values of J_{nn} and J_{nnn} in concentrated $GdCl_3$, which we would expect to be fairly close to those in our pairs, have been estimated by Boyd and Wolf[22] using specific-heat and susceptibility measurements. Unfortunately with the available data it was impossible to distinguish between two alternative pairs of solutions (A and B in Table V), but the individual J's are quite different and it should therefore be quite easy to choose between them on the basis of our pair measurements.[22a]

In addition to bilinear-isotropic exchange we may here also consider the possibility of isotropic biquadratic terms of the form $j(\mathbf{S}_1\cdot\mathbf{S}_2)^2$. Anderson[23] has estimated that j is approximately (J/U) times the usual bilinear-superexchange mechanism, where J is the bilinear-superexchange coupling constant and U the energy required to transfer an electron from an ion to a neighboring ion. Since U is probably 5–10 eV, this factor is less than 10^{-5}.

3. *Magnetic Dipole Coupling*

Values of α may readily be estimated from g and the lattice parameters given in Table I. For the pairs we would expect α to lie somewhere between the values calculated from the $LaCl_3$ and $GdCl_3$ parameters

$$\alpha_{nn}(LaCl_3)=0.0205\text{ cm}^{-1}\quad \alpha_{nnn}(LaCl_3)=0.0151\text{ cm}^{-1}$$
$$\alpha_{nn}(GdCl_3)=0.0248\text{ cm}^{-1}\quad \alpha_{nnn}(GdCl_3)=0.0163\text{ cm}^{-1}.$$

Indeed we shall use the values obtained from our final fit to estimate the effective separations of both nn and nnn pairs $r_{eff}=[g^2\mu_B{}^2/\alpha(\text{exp})]^{1/3}$. (See Sec. 6 B.) The principal uncertainty in this lies in the possibility that α may also contain a contribution from anisotropic pseudo-dipolar exchange. However, theoretical estimates[24] of

[22] E. L. Boyd and W. P. Wolf, J. Appl. Phys. **36**, 1027 (1965).

[22a] *Note added in proof*. A similar analysis based on more accurate specific heat measurements has recently been given by R. B. Clover and W. P. Wolf, Solid State Commun. (to be published). The new results clearly support solution B, in agreement with the conclusions reached in this paper.

[23] P. W. Anderson, Phys. Rev. **115**, 2 (1959); *Solid State Physics*, edited by F. Seitz and D. Turnbull (Academic Press, Inc., New York, 1963), Vol. 14, p. 99.

[24] See for example, T. Moriya, in *Magnetism*, edited by G. T. Rado and M. Suhl (Academic Press Inc., New York, 1963), Vol. 1, p. 86.

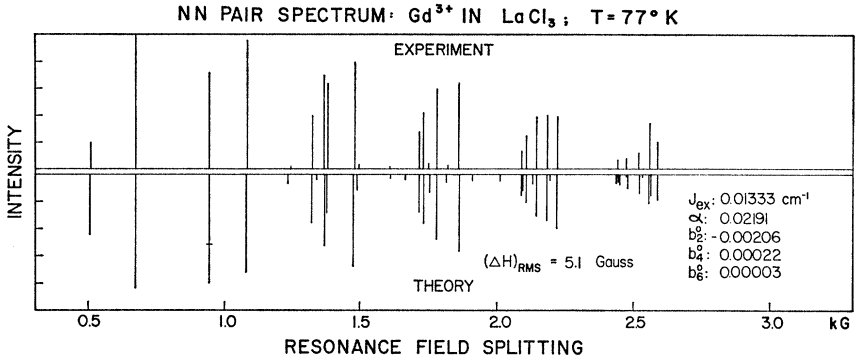

FIG. 9. Best fit to nearest-neighbor pair spectrum at $T=77°K$ with the magnetic field along the c axis.

the coefficient give $J_{an}\sim[(g_e-g)/g_e]^2J$, where g_e is the free-electron spin g value. In our case this gives $J_{an}\sim 2.10^{-6}$ cm^{-1}, which is a factor 10^4 smaller than the magnetic-dipole terms.

4. *Crystal-Field Effects*

The small crystal-field parameters found for single ions suggest strongly that crystal-field effects will generally be small also for the pairs. The actual values may be expected to vary considerably, inasmuch as they usually depend on a balance between different contributions, and we would also expect additional effects from the difference between the ionic sizes of a Gd^{3+} and La^{3+} neighbors. Moreover, in the case of a pair the point symmetry at each Gd^{3+} ion is reduced from the single ion C_{3h} symmetry and additional terms will therefore be allowed in the true crystal-field potential. Thus terms of the form Y_n^m with $m\neq 0$ or 6, and with odd as well as even n may now be present.

All terms with $m\neq 0$ will not produce any first-order shifts relative to large Zeeman splittings, and second-order effects will be asymmetric for corresponding transitions at high and low fields. The observed symmetry of the spectra shows therefore that these effects are extremely small in the present case and even if they were larger, as they will be for the Gd^{3+} pairs in $EuCl_3$ (see II) they can be eliminated by averaging the low- and high-field splittings. Symmetric third-order effects will nearly always be quite negligible.

Terms in the true crystal-field potential with n odd may quite possibly affect the spectrum through the complex high-order processes involved in the splitting of S-state ions. However such odd-n terms cannot be present in an effective Hamiltonian acting within a pure $S=\frac{7}{2}$ manifold because of inversion and time-reversal symmetry. Their higher-order effects have not been found to be observable in previously analyzed spectra of S-state single ions in low-symmetry crystal fields, and we have not included them in our analysis.

We conclude therefore that a crystal-field Hamiltonian of the form of Eq. (2) will be a very good approximation for predicting the line positions of both nn and nnn pairs, with parameters of the same general order of magnitude as these given in Table II. In practice this implies line shifts which are all much smaller than those produced by the terms in $\mathcal{H}_p^{(0)}$.

B. General Fitting Procedure

There are two major difficulties in fitting any spectrum: The correlation of the observed lines with specific transitions of a trial Hamiltonian, and the variation of the adjustable parameters to obtain a unique best fit. At first sight the fitting of over 20 lines in each half of the spectrum to the six parameters in $\mathcal{H}^{(0)}(1,2)$ here presents a formidable problem, but in fact the large number of lines proved to be a most valuable check on the final fit. Moreover, of the six parameters three (the b_n^0) are almost certainly very small and we may estimate two (g and α) with good accuracy. This effectively leaves only one unknown (J) and this may be determined directly from the value of J/α in Fig. 3 which corresponds to the observed line positions. Several different trial identifications were made and in each case the quantity $\sum_i \omega_i[H_i(\text{exp})-H_i(\text{calc})]^2$ was minimized by varying the spin-Hamiltonian parameters using a computer least-squares routine written by M. J. D. Powell.[25] Weighting factors $\omega_i=\frac{1}{2}$ were used for those lines which were poorly resolved, and $\omega_i=1$ for all others. The program was tested by calculating resonance fields for a given set of parameters and then reversing the procedure and fitting to several of them. It was found that for a given J, α, b_2^0, b_4^0, b_6^0, six to seven identifications were sufficient to determine the interaction parameters to an accuracy of 0.00001 cm^{-1}, provided that at least one of the transitions was fairly sensitive to J (see Fig. 3). If incorrect identifications were deliberately made the routine would converge but to values which gave an obviously incorrect fit.

As clues to the identifications and as criteria for the correct fit, we made the following requirements on each of the transitions: (1) the line positions must correspond, (2) the lines should have the correct relative intensity, (3) the lines must have the correct angular variation, (4) as the temperature is decreased below 4.2°K certain transitions (i.e., the low-M transitions)

[25] M. J. D. Powell, J. Comput. 7, 303 (1965).

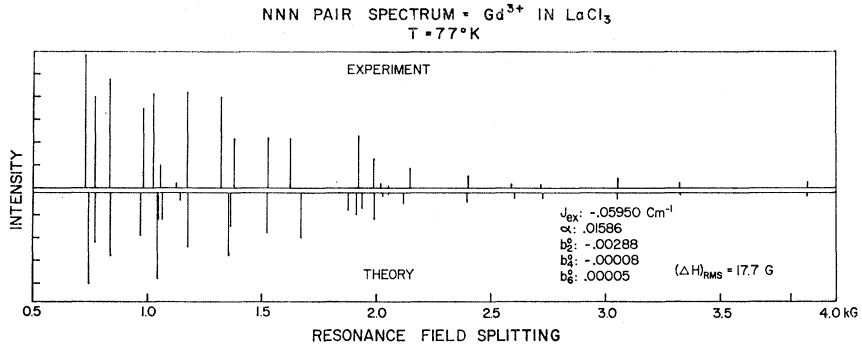

FIG. 10. Best fit to next-nearest-neighbor pair spectrum at $T=77°K$ with the magnetic field along the nnn bond axis.

should increase in intensity. In addition to these specific requirements there are also general criteria; thus, for example, the identifications must remain valid over the entire temperature range studied even though the interaction parameters may change markedly.

C. Fitting the nn Spectrum

The average nn pair experimental line positions at 77°K are shown diagramatically in the upper half of Fig. 9. Since there are no lines split by more than 2600 G from the central transition, the nn exchange must be in the central region of Fig. 3, that is $|J|\lesssim\alpha$. In fact the outstanding characteristic of the grouping of the nn lines suggests immediately that $J_{nn}/\alpha\sim\frac{1}{2}$, near the point of high degeneracy discussed in Sec. 3C. Taking $J\approx\frac{1}{2}\alpha_{nn}$ with $\alpha_{nn}\approx0.022$ cm^{-1} and using the intensities, line positions and angular variation, as clues, several identifications of lines could be made with some confidence. A series of 42 different fits were made, and it was found that one and only one set of identifications gave a good fit. This best fit is shown in the lower half of Fig. 9, and it is seen that the general agreement is excellent. The rms deviation is 5.1 G compared with linewidths of 10–20 G and splittings of up to 2600 G. In the calculation of the rms deivation very poorly resolved lines were again weighted $\frac{1}{2}$, as in the least-squares fitting. The experimental and calculated line positions are given in Table VI and it can be seen that most of the lines are in fact fitted to within the experimental error, and that the few lines with large errors are generally ones which are poorly resolved. In the label the first number is the value of $|M|$ for the initial state, and the second a computational reference number. There are a few small lines predicted between the groups which experimentally were either barely resolvable from the noise or not observed at all. These are shown in Fig. 9 but not listed in Table VI. In general however the intensities calculated on the basis of pure magnetic-dipole transitions [Eq. (6)] agreed very well with those estimated from the observed absorption derivatives.

TABLE VI. Experimental and calculated mean line splittings (in gauss) for the nn spectrum at 77°K and $\nu=25.625$ GHz, with $J=0.013333$ cm^{-1}, $\alpha=0.021911$ cm^{-1}, $b_2^0=-0.002062$ cm^{-1}, $b_4^0=0.000222$ cm^{-1}, $b_6^0=0.000027$ cm^{-1}, and $g=1.9915$.

Label	Experiment	Calculated	Difference
1, 5	512.5	512.5	−0.3
2, 1	678.7	679.3	0.6
1, 9	947.4	946.9	−0.5
2, 4	947.4	949.4	2.0
3, 1	1087.5	1084.5	−3.0
2, 8	1326.9	1322.8	−4.1
3, 4	1369.6	1371.9	2.3
1, 13	1383.2	1373.6	−9.6
4, 1	1482.7	1477.8	−4.9
1, 16	1499.5	1490.6	−8.9
2, 11	1720.0	1713.8	−6.2
3, 7	1732.7	1732.5	−0.2
1, 17	1751.8	1744.0	−7.8
4, 3	1781.7	1783.0	1.3
1, 20	1822.0	1816.0	−6.0
5, 1	1862.4	1857.5	−4.9
2, 15	2093.7	2090.6	−3.1
3, 10	2111.0	2112.0	1.0
4, 6	2187.3	2187.5	0.2
6, 1	2224.0	2220.6	−3.4
2, 18	2445.0	2454.3	9.3
1, 25	2445.0	2442.8	−2.2
1, 28	2445.0	2454.4	9.4
3, 13	2478.0	2485.4	7.4
4, 8	2522.0	2528.3	6.3
5, 5	2562.6	2570.3	7.7
7, 1	2562.6	2558.3	−4.3
6, 2	2590.3	2591.2	0.9

In Fig. 5 the angular variation calculated for the nn best-fit parameters is shown for the high-field lines together with the experimental angular variation. The general agreement is again excellent.

In order to test the presence of any intrinsic biquadratic exchange, j, this term was included in $\mathcal{H}^0(1,2)$, but it was found to improve the fit only by 0.5 G in the rms deviations. Its value, if included, was 0.00001 ($\pm$0.00002) and its presence changed the other parameters by less than 0.0002 cm^{-1}. We conclude that biquadratic exchange is certainly negligible for nn pairs.

Other small interaction and crystal-field terms neglected in $\mathcal{H}^{(0)}(1,2)$ will most probably also produce the same kinds of effects, causing line shifts of the order of the experimental uncertainty with corresponding changes in the other fitted parameters which are extremely small. We conclude therefore that the terms included in $\mathcal{H}^{(0)}(1,2)$ are determined with only small experimental uncertainties and that other interactions are orders of magnitude smaller.

The final parameters giving the best fit at 77°K are listed in Table VI and Fig. 9, the biquadratic-exchange term being set equal to zero for this fit. We note that the isotropic exchange is small and *antiferromagnetic* in sign, and that the dipolar interaction lies between values appropriate to $GdCl_3$ and $LaCl_3$ lattice spacings as we expected. The parameters and their variation with temperature will be discussed more fully in Sec. 6.

D. Fitting the nnn Spectrum

The observed high-field half of the nnn spectrum at 77°K is shown in the upper part of Fig. 10. It can be seen that, unlike the nn spectra, there are no obvious distinctive groupings or other features. However as there are a number of small transitions at splittings as great as 3900 G it seems likely from Fig. 3 that $|J| \approx 3\alpha \sim 0.05$ cm^{-1}. This is close to the second of Boyd and Wolf's estimates ($J_{\text{nnn}} \sim -0.06$ cm^{-1}), and it was found that the spacing of the more intense nnn transitions had a rough correspondence to those of Fig. 3 if J_{nnn} was near this value. Identifications were therefore made in this region using intensities and the angular variation of the lines as clues, the latter being particularly characteristic in this case. The best fit to $\mathcal{H}^{(0)}(1,2)$ was the outcome of over 60 fitting runs and is shown in the lower half of Fig. 10. As in the case of the nn's it was found that one and only one fit gave reasonable agreement. The experimental and calculated line positions are listed in Table VII, and it can be seen that the fit is generally quite good, with an over-all rms deviation of 18 G. A closer comparison does reveal that some small but significant discrepancies, and in fact only a few of the lines are fitted to within the experimental error of ±4 G, in contrast to the nn case.

These discrepancies could arise either from the fact that the identifications are simply incorrect, or that the truncated Hamiltonian in Eq. (3) is insufficient to describe the nnn pairs to better than 1%. A detailed study showed that it most certainly the latter and we shall now summarize the reasons for this conclusion.

(1) The angular variation of the high-field nnn pairs calculated from the best-fit parameters is shown in Fig. 8, together with the experimental results. The agreement between the two is remarkably good, and in fact the actual angular variation of these high-field lines is in better agreement than their positions along the bond axis, indicating that their identifications are correct. This is also supported by the angular variation of the low-field lines.

(2) The correct number of lines are predicted theoretically (this is in fact quite a stringent requirement), and their intensities correspond well with the experimental values.

(3) As the temperature was varied from 20°K to 360°K the resonance fields of the different nnn lines changed by amounts varying from −500 to +100 G. Nevertheless the identifications of Table VII gave fits with consistent rms deviations of 18.4±1.2 G over the entire temperature range. This would be highly unlikely if the identifications were incorrect. Further discussion of this point will be given in Sec. 6.

TABLE VII. Experimental and calculated mean line splittings (in gauss) for the nnn spectrum at 77°K and $\nu = 25.625$ GHz, with $J = -0.059502$ cm^{-1}, $\alpha = 0.015864$ cm^{-1}, $b_2^0 = -0.002880$ cm^{-1}, $b_4^0 = -0.000082$ cm^{-1}, $b_6^0 = 0.000050$ cm^{-1}, and $g = 1.9915$.

Label	Experiment	Calculated	Difference
3, 13	732.8	743.9	11.1
2, 11	775.4	768.0	−7.4
1, 9	775.4	777.8	2.4
3, 15	839.9	840.9	1.0
3, 7	987.3	974.8	−12.5
4, 10	1029.0	1049.0	20.0
3, 9	1061.8	1049.1	−12.7
1, 12	1131.9	1147.9	16.0
4, 8	1180.8	1177.7	−3.1
5, 5	1327.0	1359.0	32.0
4, 5	1382.5	1367.7	−14.8
5, 6	1530.7	1526.2	−4.5
6, 3	1628.2	1673.0	44.8
5, 1	1925.3	1879.0	−46.3
6, 2	1925.3	1914.3	−11.0
4, 3	1925.3	1937.7	12.4
7, 1	1992.6	1992.1	−0.5
1, 8	2023.2	2030.3	7.1
2, 10	2056.0	2062.1	6.1
3, 1	2150.2	2120.9	−29.3
2, 4	2404.3	2399.2	−5.1
1, 1	2591.0	2605.9	14.9
1, 5	2720.0	2728.1	8.1
2, 1	3056.2	3051.4	−4.8
1, 13	3315.7	3313.3	−2.4
3, 4	3882.0	3878.6	−3.4

(4) The dipolar interaction falls in the range predicted from the lattice constants and the exchange is consistent with solution (B) of Boyd and Wolf (Table V).

(5) Strong confirmation also comes from Gd^{3+} in $EuCl_3$; this will be discussed in II.

The energy-level diagram corresponding to the nnn best-fit parameters is given in Fig. 11, together with all of the transitions observed at X band. From the diagram it can be seen that several of the transitions occur almost exactly at level crossings and therefore some anomalous behavior is expected. Thus it was found that anomalies such as the absence of the high-field lines at $\Delta H \simeq 1380$ G and $\Delta H \simeq 1325$ G can be explained by the fact that they are predicted to occur very close to crossings between two energy levels which are connected by off-diagonal crystal-field terms. The corresponding transitions at K band do not occur near crossings and are observed as predicted.

We therefore conclude that a Hamiltonian including only isotropic exchange, dipolar interaction and the *diagonal* crystal-field terms is sufficient to describe the nnn pair-resonance positions to ~1% but no better than this. In the next subsection we shall discuss various possible additional terms although in fact none of these appear to be able to account for the discrepancies, which thus remain somewhat puzzling. However, judging from the general effects of small additional terms it seems

TABLE VIII. Final values of nn and nnn parameters for 77°K, compared with the calculated dipolar constants for $GdCl_3$ and $LaCl_3$ lattice spacings and single-ion effective crystal-field parameters. The parameters are defined in Eq. (3). All energies are expressed in cm^{-1}.

		g	J	α	b_2^0	b_4^0	b_6^0
nn pairs	nn pair spectrum	1.9915 (±0.0010)	0.0133 (±0.0005)	0.0219 (±0.0003)	−0.00206 (±0.00020)	0.00022 (±0.00005)	0.00003 (±0.00001)
	Calc. $\{(LaCl_3)$	...	...	0.0207[a]	...	...	...
	Calc. $\{(GdCl_3)$			0.0250[a]			
	Single ion	1.9915 (±0.0006)	...	...	0.00160 (±0.00002)	0.000213 (±0.000005)	0.000025 (0.000005)
nnn pairs	nnn pair spectrum	1.9915 (±0.0010)	−0.0595 (±0.0020)	0.0159 (±0.0005)	−0.0029 (±0.0015)	−0.00008 (±0.00003)	0.00005 (±0.00003)
	Calc. $\{(LaCl_3)$	...	...	0.0153[a]	...	...	...
	Calc. $\{(GdCl_3)$			0.0166[a]			
	Calculated from rotation of single-ion values	...	...	...	−0.0003	−0.00005	0.0000

[a] Calculated for $g=1.9915$ and lattice parameters given in Table I reduced to allow for thermal contraction at 77°K.

most unlikely that the values of the six principal parameters which we have fitted so far will be altered significantly in any more refined fit and we therefore list them with correspondingly small errors in Table VIII. The discussion of the parameters and their variation with temperature is deferred until Sec. 6.

E. Discussion of the nnn Discrepancies

In this subsection we discuss several attempts to account for the remaining small discrepancy between the nnn calculated and experimental line positions. We have seen that it is an experimental fact that the spectrum is symmetric about the central single-ion transition and about the bond axis if the angle is varied, and that the relative pair line positions are independent of frequency to a very good approximation. Furthermore the experimental line positions in Table VII are all averages over high- and low-field pairs, and should thus average out any small second-order shifts. Any further terms added to $\mathcal{H}^{(0)}(1,2)$ to remove the discrepancies must therefore commute with T_z, as any off-diagonal terms would primarily cause an asymmetry. We can therefore rule out as extremely unlikely the effects due to off-diagonal crystal-field terms.

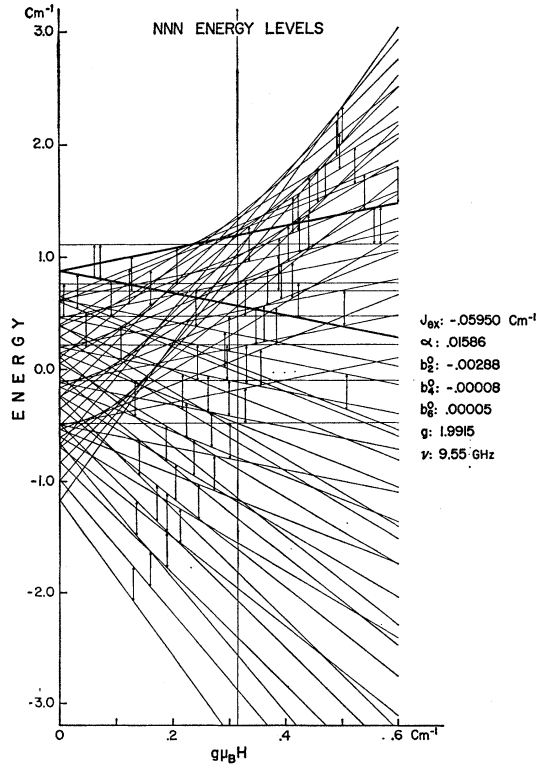

FIG. 11. Energy-level diagram for the next-nearest neighbor pairs at $T=77$°K. Each of the arrows correspond to transitions observed at X band. The vertical line corresponds to the center of the spectrum.

Considering the interaction terms, we may note that it is highly unlikely that there is any coupling mechanism which acts between the nnn which does not act between the nn as well, unless it is one which is forbidden by the symmetry of the nn pairs but is allowed by the low symmetry about the nnn pair axis. We have already included all the bilinear terms commuting with T_z in $\mathcal{H}^{(0)}(1,2)$ except for the diagonal antisymmetric terms in the Dzhialoskinski-Moriya interaction, $d_z(S_{x1}S_{y2}-S_{y1}S_{x2})$. These are ruled out by symmetry in the undistorted trichloride lattice, but it is conceivable that a small displacement of the ions around a nnn pair could remove the center of inversion. However in practice the inclusion of a term of this form gave no improvement in the fit, and we conclude that d_z must be extremely small.

Possible biquadratic-interaction terms which commute with T_z have the form

$$\mathcal{H}_p{}^{bq}=j(\mathbf{S}_1\cdot\mathbf{S}_2)^2+j'(S_{z1}S_{z2}\mathbf{S}_1\cdot\mathbf{S}_2+\mathbf{S}_1\cdot\mathbf{S}_2S_{z1}S_{z2}) +j''S_{z1}{}^2S_{z2}{}^2. \quad (9)$$

These were tried first with $j'=j''=0$ corresponding to the isotropic exchange form and then with all three terms, but none of these terms appeared to substantially improve the fit. Indeed from theoretical considerations we would expect them to be very small.

Another higher-order mechanism which we have con-

sidered is an interaction-induced distortion effect. This has been found to occur in the case of Mn^{2+} pairs in MgO[26] and takes a somewhat similar, although distinct, form to the higher-order terms given above. Indeed for the special case of large intrinsically isotropic interactions it produces extra terms in the spin Hamiltonian which have exactly the same form as those already considered, namely $j(\mathbf{S}_1\cdot\mathbf{S}_2)^2$. However for the present case where other interactions such as magnetic-dipole terms are present, it cannot be accounted for by the terms in Eq. (9).

The effect arises from the fact that the exchange and dipolar interactions are separation dependent, and therefore for a given spin state the relative separation of the pairs will change so as to minimize the sum of the magnetic and the elastic energies. Let us consider the particular case where the change in separation is along the pair axis, and use the harmonic approximation for the elastic energy, $\delta E_{\text{elastic}}=\frac{1}{2}cx^2$, where c is an elastic constant and x is the change from the equilibrium separation. Minimizing the sum $\langle i|\mathcal{H}_{12}(x)|i\rangle+\delta E_{\text{elastic}}$ with respect to x, one may then show that the change of energy of the ith state of the pair due to the distortion is

$$\begin{aligned}\Delta E_i=&-(1/2c)[(\partial J/\partial x)^2+2(\partial\alpha/\partial x)(\partial J/\partial x)+(\partial\alpha/\partial x)^2]\\&\times\langle i|\mathbf{S}_1\cdot\mathbf{S}_2|i\rangle^2-(9/2c)[(\partial\alpha/\partial x)]^2\langle i|S_{z1}S_{z2}|i\rangle^2\\&+(3/c)[(\partial\alpha/\partial x)^2+(\partial J/\partial x)(\partial\alpha/\partial x)]\\&\times\langle i|S_{z1}S_{z2}|i\rangle\langle i|\mathbf{S}_1\cdot\mathbf{S}_2|i\rangle. \quad (10)\end{aligned}$$

Providing the lattice can relax in a time short compared with the microwave frequency, as seems likely, these additional level shifts will be observed in a resonance measurement. To estimate an order of magnitude of the effect in our case we take $c\sim3\times10^{19}\sim\text{cm}^{-1}/\text{cm}^2$, $|\partial J/\partial x|\sim2.5\times10^7$ cm^{-1}/cm and $|\partial\alpha/\partial x|\sim1\times10^6$ cm^{-1}/cm. We then find $\Delta E_i\sim5$ G, which is somewhat smaller than the observed discrepancies. However as it is generally difficult to estimate magnitudes of effects of this kind, a number of fitting runs including the terms in Eq. (10) were made treating c and $\partial J/\partial x$ as adjustable parameters. Unfortunately no significant improvement to the fit was obtained, and we must conclude that magneto-elastic effects are really not important in this case.

It seems therefore that the 1% discrepancy in the nnn fit is not explained by any of the conventional higher-order coupling mechanisms and it does not seem to be due to the off-diagonal crystal-field terms. Thus we seem to require a new small (higher-order) coupling mechanism, of the order of $\frac{1}{10}$ to 1% of the isotropic exchange, which is diagonal in $S_{z1}+S_{z2}$ and which contributes only in cases of very low symmetry. So far we have not been able to find any specific mechanism which has these properties. However the effects are very small and could well be due to complex higher-order interactions involving for example cross terms between electric-multipole interactions and spin-orbit coupling.

[26] E. A. Harris (private communication).

6. DISCUSSION OF THE MEASURED PARAMETERS AND THEIR TEMPERATURE VARIATION

The pair parameters measured at 77°K are summarized in Table VIII together with some related results for comparison. The errors given in Table VIII are estimates of the over-all accuracy, taking into account both experimental errors and the uncertainties produced by the omission of the various small or unknown terms in $\mathcal{H}^{(0)}(1,2)$. The relative accuracy with which we can determine changes in the fitted parameters is very much higher, being limited only by field measurements, and this has made it possible for us to measure significant changes in all the parameters as a function of temperature. For changes in α_{nn} and α_{nnn} the relative accuracy is about $\pm4\times10^{-5}$ cm^{-1}, while for changes in J_{nn} and J_{nnn} it is of the order of $\pm10^{-4}$ and $\pm10^{-3}$ cm^{-1}, respectively.

Below 77°K the interactions do not change appreciably and we may therefore discuss them first in terms of intrinsic interaction mechanisms which will also be important for the ferromagnetic ordering of $GdCl_3$ at 2.2°K. In the following subsection we shall then discuss the variation of the interactions with temperature which depend on additional lattice-vibration effects.

A. Low-Temperature Results

One of the principal results of our experiments is the verification of the fact that the form of the interactions between two Gd^{3+} ions is dominated by an isotropic bilinear (exchange) term plus magnetic-dipole coupling consistent with the known lattice spacings. From a theoretical point of view the highly isotropic nature of the exchange is not entirely trivial, since it is the result of a large number of different anisotropic-superexchange interactions, which add up to a scalar form only because the Gd^{3+} ground state is almost completely an S state. For such a case VanVleck has shown[7] that even anisotropic individual electron exchange terms will add to give a total interaction of the form $\mathbf{S}_1\cdot\mathbf{S}_2$.

The second, and perhaps more surprising result, concerns the relative magnitudes and signs of J_{nn} and J_{nnn}. In the absence of any detailed theoretical predictions, it was not at all clear which of the two would be dominant, and in the earliest work[11] on $GdCl_3$ the seemingly reasonable assumption was made that $|J_{\text{nn}}|\gg|J_{\text{nnn}}|$, with $J_{\text{nn}}<0$ to account for the observed ferromagnetism. Our results here show clearly that this is not the case and that the dominant interaction is a ferromagnetic coupling between next-nearest neighbors. The coupling between nearest neighbors is found to be much weaker and antiferromagnetic in sign, in general agreement with the second solution of Boyd and Wolf[22] (see Table V).[22a]

Although at first somewhat surprising, the larger nnn coupling is in fact not unreasonable on a superexchange

TABLE IX. Temperature dependence of the interaction constants for nn pairs of Gd^{3+} in $LaCl_3$.

Temperature (°K)	J_{nn} (cm^{-1})	α_{nn} (cm^{-1})	b_2^0 (cm^{-1})	b_4^0 (cm^{-1})	b_6^0 (cm^{-1})	$(\Delta H)_{rms}$ (G)
20	0.01330	0.02193	−0.00201	0.00021	0.00003	5.3
77	0.01333	0.02191	−0.00201	0.00022	0.00003	5.1
145	0.01311	0.02187	−0.00216	0.00021	0.00003	4.7
195	0.01293	0.02181	−0.00225	0.00022	0.00003	3.8
207	0.01286	0.02179	−0.00230	0.00022	0.00003	3.8
243	0.01280	0.02175	−0.00234	0.00022	0.00004	3.9
265	0.01274	0.02172	−0.00240	0.00023	0.00003	3.9
295	0.01268	0.02169	−0.00242	0.00024	0.00004	4.2
329	0.01259	0.02165	−0.00247	0.00025	0.00004	4.6
361	0.01254	0.02162	−0.00250	0.00026	0.00004	4.9

model in which the interaction takes place via the intervening Cl^- ions. Measured directly, the distances between the nn and nnn are 4.28 and 4.77 Å, respectively but the superexchange paths Gd^{3+}–Cl^-–Gd^{3+} are much more similar, being $A+A=5.88$ Å for the three nn bonds and $A+B=5.90$ Å for the two nnn bonds (see Table I). The bond angles Gd^{3+}–Cl^-–Gd^{3+} are 96° and 110°, respectively, and thus the nnn do in fact have a more direct path. The relatively small nn interaction could also result from a partial cancellation of the individual electron-electron contributions. We have made no attempt to explain our results in detail as all realistic calculations would necessarily be very complex. However, we do believe that the problem is clear enough to warrant such a calculation, and our parameters together with their variation with temperature and host lattice should provide critical checks on the results.

The crystal-field parameters likewise present a complex problem which requires quite detailed calculations, but if we compare the values of the b_n^0 given in Table VIII several significant features are immediately apparent. Firstly, the parameters are all relatively small justifying the original assumption which proved to be a major aid in the fitting of the spectra. Secondly, we may note that the largest terms for both nn and nnn are the b_2^0 which are of comparable magnitude but opposite sign to the single-ion b_2^0. The b_4^0 and b_6^0 on the other hand are very small and quite similar to the single-ion values. This indicates that only the b_2^0 are affected significantly by the neighboring Gd^{3+} ion in the pair. From a practical point of view this is useful as it ensures that the crystal field for the nnn pairs is dominated by a single term, which moreover has axial symmetry about the pair axis, as in our truncated crystal-field Hamiltonian, $V_c^{(0)}$ [Eq. (2)].

B. Temperature Variation

The results of fitting nn and nnn spectra at ten fixed temperatures between 20 and 360°K are summarized in Tables IX and X.[27] It may be seen that all the parameters vary smoothly within the small uncertainties of the analysis, and that the rms deviations remain essentially constant throughout. The crystal-field parameters remain very small over the whole temperature range, as we might expect, with b_2^0 dominant in all cases, but the exchange and dipole interactions show significant decreases as the temperature is raised. The variation of J_{nn} and J_{nnn} with temperature is shown in Fig. 12. Above about 150°K the curves are approximately linear with gradients $[(1/J)(dJ/dT)]_{nn}\sim-1.8\times10^{-4}$ (°K)$^{-1}$, $[(1/J)(dJ/dT)]_{nnn}\sim-4.3\times10^{-4}$ (°K)$^{-1}$. These are somewhat larger than previous estimates (1 to 2×10^{-4}) for various ferric oxide garnets and spinels based on analyses of bulk measurements.[28] The dipolar constants, α_{nn} and α_{nnn}, also vary with temperature, but much more slowly, with gradients $[(1/\alpha)(d\alpha/dT)]_{nn}\sim-0.5\times10^{-4}$ (°K)$^{-1}$, and $[(1/\alpha)(d\alpha/dT)]_{nnn}\sim-0.7\times10^{-4}$ (°K)$^{-1}$, consistent with a coefficient of thermal expansion $\sim2\times10^{-5}$ (°K)$^{-1}$. The variation of the exchange interactions is generally important for the interpretation of high-temperature magnetic data, where it can lead to incorrect values of the deduced Curie constant.[28] In the present case the effect will be small because the J's are small, but in other cases values of $(1/J)(dJ/dT)$ similar to those found here could be quite important.

The temperature dependence of the exchange interactions may be interpreted in terms of two effects resulting from the increased amplitude of the lattice vibrations: (1) anharmonic thermal expansion effects and (2) harmonic-vibration effects. Both effects may be visualized quite readily in general terms, although

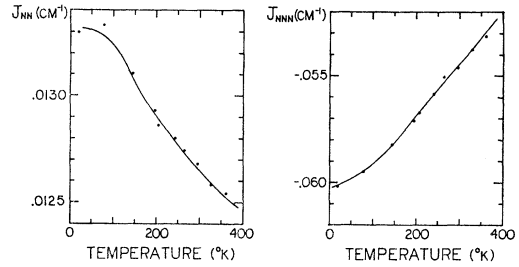

FIG. 12. Temperature variation of J_{nn} and J_{nnn}.

[27] Measurements were also made at 1.6 and 4.2°K but at these lower temperatures the lines were very broad probably because of saturation.

[28] L. Néel, J. Phys. Radium **12**, 258 (1951); R. Pauthenet and P. Blum, Compt. Rend. **239**, 33 (1954); R. Aléonard and J. C. Barbier, *ibid.* **245**, 831 (1957).

TABLE X. Temperature dependence of the interaction constants for nnn pairs of Gd^{3+} in $LaCl_3$.

Temperature (°K)	J_{nnn} (cm^{-1})	α_{nnn} (cm^{-1})	b_2^0 (cm^{-1})	b_4^0 (cm^{-1})	b_6^0 (cm^{-1})	$(\Delta H)_{rms}$ (G)
20	−0.06017	0.01587	−0.00292	−0.00009	0.00006	18.5
77	−0.05950	0.01586	−0.00288	−0.00008	0.00005	17.7
145	−0.05824	0.01583	−0.00271	−0.00011	0.00006	17.9
195	−0.05709	0.01578	−0.00265	−0.00011	0.00005	17.8
207	−0.05673	0.01579	−0.00254	−0.00009	0.00007	17.2
243	−0.05588	0.01577	−0.00246	−0.00009	0.00007	18.2
265	−0.05504	0.01572	−0.00242	−0.00010	0.00006	18.0
295	−0.05463	0.01568	−0.00255	−0.00012	0.00006	17.9
329	−0.05375	0.01565	−0.00246	−0.00012	0.00007	18.7
361	−0.05317	0.01561	−0.00237	−0.00012	0.00005	19.6

detailed calculations would be very difficult. The first, and presumably dominant effect arises from the increase in the mean separations between the ions with corresponding changes in the superexchange paths, which generally decrease the exchange constants. The changes in the mean separations could in principle be measured by x-ray diffraction, or, as we shall see, from the observed magnetic-dipole interactions. The second effect may be viewed as a weighted averaging of the separation-dependent exchange by the thermal (and zero-point) lattice vibrations.[29] In general this may be expected to *increase* the average-value of interactions which fall off with increased separation, but in the case of a superexchange interaction the effect may be complicated by the relative motions of cations and anions. However with typical lattice amplitudes (~0.1 Å at room temperature) the modulation effects will probably be small, and we conclude tentatively that the changes in the mean separations are more important than the modulations about the mean. This is at least consistent with the observed decrease of both J_{nn} and $|J_{nnn}|$ in our case.

If we make the extreme assumption that the modulation effects are in fact negligible, we may make a direct comparison between the changes in the α's and the J's, which may be expressed in terms of a dependence of the J's on the effective mean separations between the ions in the pairs. Treating the α's as due to purely magnetic interactions between static dipoles, we have $\alpha=g^2\mu_B^2/r_{eff}^3$, from which the effective separation r_{eff} may readily be found. The values obtained in this way are given in Table XI. In addition to the effects of lattice vibrations, the principal uncertainty in these values is the possibility of a contribution of anisotropic exchange to the α's, but as discussed before (Sec. 5A) this will be very small in our case. In any case, we expect the changes in r_{eff} as detected from the change in α to be accurate, even if the absolute value is not.

Subject to these assumptions, we may now express the temperature dependence of the J's in terms of variations with r_{eff}. The results may be summarized by approximate logarithmic derivatives

$$x_{nn}=\frac{d(\ln|J_{nn}|)}{d(\ln r_{nn})}=-13\pm4 \tag{11}$$

$$x_{nnn}=\frac{d(\ln|J_{nnn}|)}{d(\ln r_{nnn})}=-22\pm6. \tag{12}$$

The difference between these derivatives is striking, as is the very large value for x_{nnn}, although a value almost as large (17±6) has recently been reported for EuO.[30] The value for x_{nnn} is in clear contradiction with the recently proposed 10th power law for superexchange.[31] However we must note that the mean separation between the cations is really not a very significant parameter, as illustrated dramatically by the difference between J_{nn} and J_{nnn}, and in the absence of any detailed superexchange calculation we can only draw the obvious qualitative conclusion that the exchange interactions are very sensitive to the lattice parameters.

From a practical point of view this immediately raises an important question concerning the applicability of the pair results to concentrated $GdCl_3$ which has appreciably smaller lattice constants than the present $LaCl_3$ host lattice. If we use the relations given in Eqs. (11) and (12) to make rough empirical extrapolations to the separations corresponding to pure $GdCl_3$, we find $J_{nn}(GdCl_3)=0.023$ cm^{-1} and $J_{nnn}(GdCl_3)=-0.073$ cm^{-1}, compared with our uncorrected pair values $J_{nn}(LaCl_3)=0.013\,cm^{-1}$ and $J_{nnn}(LaCl_3)=-0.060\,cm^{-1}$. We see that the changes are significant but that the *qualitive* conclusions regarding the relative magnitudes and signs are unaltered.

On the other hand it is also clear that the pair parameters can only be applied quantitatively to concentrated $GdCl_3$ if the rather large extrapolation can be made accurately, and this requires additional information on the variation with lattice parameters. Such information can fortunately be obtained from additional experiments using $EuCl_3$ as host lattice and these are described in a following paper (II). We shall therefore defer the detailed comparison of the pair measurements

[29] The effective averaging depends on the fact that the frequencies of the lattice vibrations are much higher than the measuring frequencies, but slow compared with electron-transfer times.

[30] D. A. McWhan, P. C. Sauers, and G. Jura, Phys. Rev. **143**, 385 (1966).

[31] D. Bloch, J. Phys. Chem. Solids **27**, 881 (1966).

TABLE XI. Temperature dependence of exchange and dipolar constants for nn and nnn pairs of Gd^{3+} in $LaCl_3$.

Temperature (°K)	J_{nn} (cm^{-1})	α_{nn} (cm^{-1})	r_{nn} (Å)	J_{nnn} (cm^{-1})	α_{nnn} (cm^{-1})	r_{nnn} (Å)
20	0.01330±10	0.02193±3	4.278±2	−0.0602±10	0.01587±5	4.765±3
77	0.01333	0.02191	4.279	−0.0595	0.01586	4.766
145	0.01310	0.02187	4.282	−0.0582	0.01582	4.769
195	0.01293	0.02181	4.286	−0.0571	0.01578	4.774
207	0.01286	0.02179	4.287	−0.0567	0.01579	4.773
243	0.01280	0.02175	4.290	−0.0559	0.01576	4.776
265	0.01274	0.02172	4.292	−0.0550	0.01572	4.780
295	0.02168	0.02169	4.294	−0.0546	0.01567	4.875
329	0.01258	0.02165	4.296	−0.0538	0.01565	4.787
361	0.01254	0.02162	4.299	−0.0532	0.01561	4.791

with other results, but for the present we may note that the general agreement with earlier analyses of bulk data is at least satisfactory, and it clearly resolves the ambiguity between two alternative interpretations.

7. SUMMARY AND CONCLUSION

The series of measurements described in this paper have demonstrated that very precise values of exchange and dipolar interactions may be obtained from the EPR spectra of coupled pairs of ions when the two interactions are of comparable magnitude. A general graph giving the line positions of the stronger transitions of two interacting $S=\frac{7}{2}$ spins for different exchange and dipolar interactions has been presented and used to identify the spectra due to nearest- and next-nearest neighbor Gd^{3+} pairs in $LaCl_3$. An accurate fit to both spectra is obtained by including small axial crystal-field terms and a number of possible additional interactions are discussed. For the next-nearest neighbor pairs there appear to be some very small (~1%) systematic discrepancies which are not explained and which seem to indicate some neglected higher-order interaction terms. However the major part of the interactions is well accounted for by the usual Heisenberg form of the exchange plus magnetic-dipole interaction, and the exchange constants J can be determined to an absolute accuracy of better than ±5%.

The results for the nearest-neighbor pairs show that the nearest-neighbor exchange is relatively weak and *anti*ferromagnetic while the next-nearest neighbor exchange is four times stronger and ferromagnetic, removing the ambiguity in earlier speculations based on bulk measurements. The values of the parameters have been discussed in Sec. 6, but we have not been able to find any fundamental explanation for their magnitudes nor even their signs, which remain as an apparently fruitful problem for detailed superexchange calculations.

For S-state ions such as Gd^{3+} EPR can generally be observed over a wide range of temperatures and in principle it should therefore be possible to study the changes of the effective interactions with temperature from the corresponding variation of the pair spectra. However such changes are generally small and with the usual intensity method of determining exchange constants from pair spectra it is hard to obtain sufficient accuracy. In the present case, on the other hand, the relative accuracy is so high that changes of the order of 1% can easily be detected, and we have therefore been able to measure the temperature dependence of the exchange and dipolar constants from 20° to 360°K. The over-all change of J_{nn} is -0.00076 cm^{-1} (6%) and that of J_{nn} is 0.0070 cm^{-1} (12%). From the results we can obtain some approximate estimates for the corresponding variations of the exchange constants with the mean separation between neighbors, and we find extremely rapid variations which emphasize the care which must be used in extrapolating interaction parameters from one lattice to another. The extrapolation of the present pair results to concentrated $GdCl_3$ will be discussed in a following paper which relates the present results to a similar series of measurements on Gd^{3+} pairs in $EuCl_3$.

ACKNOWLEDGMENTS

We are extremely grateful to Dr. G. Garton, S. Itzkovitz, and S. Mroczkowski for providing the crystals and assisting with their orientation, and we would like to thank Dr. J. M. Baker, Dr. M. Blume, Dr. E. A. Harris, and Dr. M. E. Lines for a number of helpful discussions. We are also indebted to M. J. D. Powell for the kind loan of his special parameter-fitting program, and to L. Hanson for assistance with some of the experiments.